







RESEARCH

Open Access



Harmonised culture procedures minimise but do not eliminate mesenchymal stromal cell donor and tissue variability in a decentralised multicentre manufacturing approach

Sandra Calcat-i-Cervera^{1†}, Erika Rendra^{2†}, Eleonora Scaccia^{2†}, Francesco Amadeo^{3,4,5†}, Vivien Hanson⁴, Bettina Wilm^{3,5}, Patricia Murray^{3,5}, Timothy O'Brien^{1,6}, Arthur Taylor^{3,5†} and Karen Bieback^{2,7*†}

Abstract

Background Mesenchymal stromal cells (MSCs), commonly sourced from adipose tissue, bone marrow and umbilical cord, have been widely used in many medical conditions due to their therapeutic potential. Yet, the still limited understanding of the underlying mechanisms of action hampers clinical translation. Clinical potency can vary considerably depending on tissue source, donor attributes, but importantly, also culture conditions. Lack of standard procedures hinders inter-study comparability and delays the progression of the field. The aim of this study was A- to assess the impact on MSC characteristics when different laboratories, performed analysis on the same MSC material using harmonised culture conditions and B- to understand source-specific differences.

Methods Three independent institutions performed a head-to-head comparison of human-derived adipose (A-), bone marrow (BM-), and umbilical cord (UC-) MSCs using harmonised culture conditions. In each centre, cells from one specific tissue source were isolated and later distributed across the network to assess their biological properties, including cell expansion, immune phenotype, and tri-lineage differentiation (part A). To assess tissue-specific function, angiogenic and immunomodulatory properties and the in vivo biodistribution were compared in one expert lab (part B).

Results By implementing a harmonised manufacturing workflow, we obtained largely reproducible results across three independent laboratories in part A of our study. Unique growth patterns and differentiation potential were observed for each tissue source, with similar trends observed between centres. Immune phenotyping verified expression of typical MSC surface markers and absence of contaminating surface markers. Depending on the established protocols in the different laboratories, quantitative data varied slightly. Functional experiments in part B concluded that conditioned media from BM-MSCs significantly enhanced tubulogenesis and endothelial migration in vitro. In contrast, immunomodulatory studies reported superior immunosuppressive abilities for A-MSCs. Biodistribution studies in healthy mice showed lung entrapment after administration of all three types of MSCs, with a significantly faster clearance of BM-MSCs.

[†]Sandra Calcat-i-Cervera, Erika Rendra, Eleonora Scaccia, Francesco Amadeo, Arthur Taylor and Karen Bieback contributed equally

*Correspondence:

Karen Bieback

Karen.Bieback@medma.uni-heidelberg.de

Full list of author information is available at the end of the article



© The Author(s) 2023. **Open Access** This article is licensed under a Creative Commons Attribution 4.0 International License, which permits use, sharing, adaptation, distribution and reproduction in any medium or format, as long as you give appropriate credit to the original author(s) and the source, provide a link to the Creative Commons licence, and indicate if changes were made. The images or other third party material in this article are included in the article's Creative Commons licence, unless indicated otherwise in a credit line to the material. If material is not included in the article's Creative Commons licence and your intended use is not permitted by statutory regulation or exceeds the permitted use, you will need to obtain permission directly from the copyright holder. To view a copy of this licence, visit <http://creativecommons.org/licenses/by/4.0/>. The Creative Commons Public Domain Dedication waiver (<http://creativecommons.org/publicdomain/zero/1.0/>) applies to the data made available in this article, unless otherwise stated in a credit line to the data.

Conclusion These results show the heterogeneous behaviour and regenerative properties of MSCs as a reflection of intrinsic tissue-origin properties while providing evidence that the use of harmonised culture procedures can reduce but do not eliminate inter-lab and operator differences.

Keywords Mesenchymal stromal cells (MSCs), Tissue source, Multicentre comparison, Manufacturing, Harmonisation, Angiogenesis, Immunomodulation, In vivo distribution

Background

Mesenchymal stromal cells (MSCs) are multipotent cells that have attracted huge interest in different areas of regenerative medicine. Because of their unique immunomodulatory, anti-inflammatory and pro-regenerative abilities [1–3], their ease of isolation from multiple tissues [4] and high expansion potential *ex vivo*, MSCs have been extensively studied in several pre-clinical models and early phase clinical trials to treat a variety of human diseases [1, 5].

MSCs were first isolated from bone marrow (BM-) in 1968 by Friedenstein et al. [6] and since then cells with similar properties have been identified in several other tissues (e.g. adipose tissue, umbilical cord, skin tissue) [4]. Although BM-MSCs are the most commonly used cell source in clinical trials [7], adipose (A-) and umbilical cord (UC-) derived MSCs have become quite attractive sources as they can be easily obtained with relatively good yields and less invasively [8]. The possibility to isolate MSCs from different starting materials elicits the question of whether it is more advantageous to use autologous or allogeneic cells. The use of autologous MSCs guarantees an easy source that does not evoke allo-immunity. However, it is associated with high costs of isolation, expansion, safety testing and donor-related comorbidities that might impact product quality [7]. Allogeneic cells may offer a more cost-effective and better standardisable off-the-shelf product. Hence, merging knowledge about basic cell characteristics (viability, proliferation, immunophenotype) together with bioactivity in a range of assays could help in identifying the ‘right’ source for the ‘right’ application.

Unfortunately, despite years of research and highly promising preclinical data, the translation to the clinic is well below expectations. In many clinical trials, MSCs have shown little benefit [1, 5, 9]. Inconsistent and poorly defined manufacturing procedures increase the heterogeneity that intrinsically exists in a field where donor variability and tissue origin have a strong role. Thus, when considering clinical translation, defining an optimal scalable manufacturing workflow is key to ensure product quality while minimising costs and timelines [10]. Numerous different manufacturing workflows have been established, which largely affect cell characteristics. Stroncek and colleagues recently demonstrated that variations in cell culture procedures affected the functional

and molecular characteristics of the cells to a much higher extent than the source material itself, which was shipped across five different manufacturing centres [11]. The variation in culture conditions included the use of different media (type and composition), sera (origin and concentration in the medium) and seeding densities [11]. This emphasised that clinical-scale manufacturing requires optimisation, and importantly, worldwide harmonisation/standardisation.

Within the context of the RenalToolBox EU ITN Network [<https://www.renaltoolbox.org>], which includes several leading EU academic institutions and industry experts, researchers from the University of Liverpool (Liverpool, UK), the University of Heidelberg (Heidelberg, Germany) and the University of Galway (Galway, Ireland) collaborated to assess biological and therapeutic properties of MSCs derived from bone marrow (BM-MSC), adipose tissue (A-MSC), and umbilical cord (UC-MSC) in a multicentre comparative study. In part A of our study, we focused on comparing cell characteristics across centres using harmonised culture conditions for A-, BM- and UC-MSCs mimicking three decentralised manufacturing sites. MSCs were generated in one centre, shipped as cryo-aliquots to the other centres and cultivated under harmonised standard culture conditions to compare cell behaviour, differentiation potential and expression of MSC markers *in vitro* (Fig. 1).

Assessing the impact of harmonised manufacturing methods on biological properties beyond basic cell characterisation could provide helpful insights to decipher particular mechanisms of action of different tissue-origin MSCs. Thus, in part B, we assessed tissue source specificities further. Given that some of their therapeutic properties are elicited by their ability to release soluble bioactive factors to promote angiogenesis as well as to modulate immune responses [12–14], these properties were assessed individually in Galway and Heidelberg, respectively. The team in Liverpool compared the *in vivo* biodistribution in a small rodent model (Fig. 1).

Materials and methods

Mesenchymal stromal cells culture

MSCs were obtained from different sites participating in the RenalToolBox network. A-MSCs from lipospirates

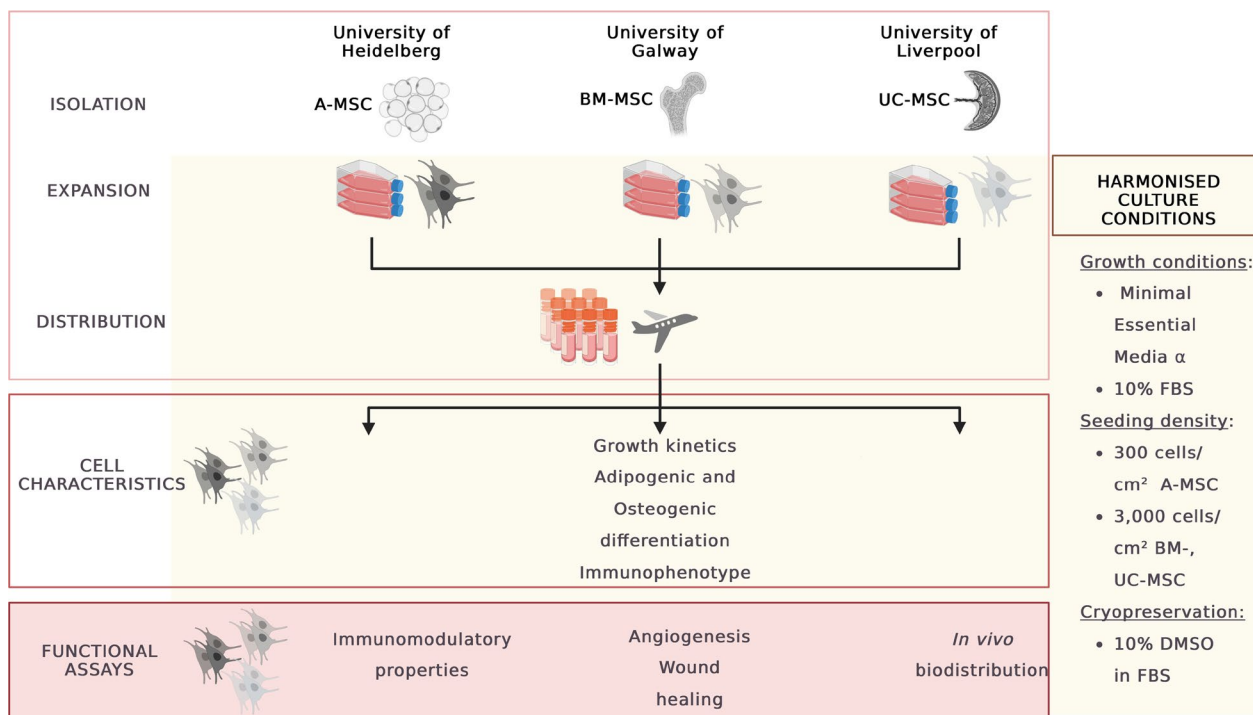


Fig. 1 Schematic representing study design and assay distribution across centres

(healthy donors of both gender in a range of age 47–25 years) were processed in Heidelberg after obtaining informed consent (title of approved project: isolation and characterisation of MSCs from human adipose tissue; institutional approval committee: Mannheim Ethics Commission II; approval number: 2006-192N-MA; date of approval: 18.04.2005, re-confirmed 26.02.2009 with subsequent approvals). BM-MSCs provided by Galway were isolated from bone marrow aspirates (healthy young male donors) purchased from Lonza (Basel, Switzerland) (title of approved project: Isolation of Human Marrow Stem Cells from Healthy Donors; Bone Marrow Research Study”, institutional approval committee: Galway University Hospital Clinical Research Ethics Committee; approval number: 02/08; date of approval: November 2008 with subsequent approvals for amendments). UC-MSCs with informed consent obtained in accordance with the Declaration of Helsinki were sourced from the NHS Blood and Transplant and transferred to the University of Liverpool (project title: the provision of mesenchymal stromal cells to the University of Liverpool for use in the RenalToolBox project; institutional approval unit: NHS Blood and Transplant, Cellular and Molecular Therapies; approval number: RTB21112019; date of approval: 21 November 2019). Three different donors per tissue source were isolated in each centre according to their standard procedures ([15] Galway, [16]

Heidelberg). From passage 3 (A- and BM-MSCs) or passage 4 (UC-MSCs), cells were expanded using harmonised conditions (see supplementary data) and banked prior to distribution across the network (see below). After shipment and subsequent storage in liquid nitrogen, MSCs were thawed and cultivated under defined harmonised conditions. These included the basic growth medium (MEM-α media, Gibco, ThermoFisher Scientific), a common lot of foetal bovine serum (FBS, Gibco, ThermoFisher Scientifics, Cat-No. 10,270–106, Lot 42Q7096K) and optimised seeding densities (300 cells/cm² for A-MSCs and 3,000 cells/cm² for BM- and UC-MSCs) at 37 °C with 5% (v/v) CO₂ and controlled humidity (see supplementary data for more information on FBS batch testing and seeding densities). All experiments were performed within a similar passage number, ranging from p4 to p6 depending on experimental requirements and intrinsic factors such as initial availability.

Cryopreservation

Upon reaching 70% confluency, MSCs were cryopreserved for distribution across sites. Cells were dissociated by trypsinisation (0.25% Trypsin-Ethylenediaminetetraacetic Acid 1X, Gibco, ThermoFisher Scientific, 25,200–056), counted using appropriate methods (NucleoCounter NC-200 automated cell counter (Galway), CASY cell counter with dead cell exclusion

(Heidelberg), manual cell counting (Liverpool)) and centrifuged. Between 5×10^5 and 1×10^6 cells/ml were resuspended in freezing media (FBS + 10% Dimethyl Sulfoxide, DMSO, Sigma, D2660) and frozen down.

Conditioned media collection

Conditioned media (CM) were generated from MSCs at passage 4 to 6. Upon reaching 80% confluency, cells were washed with 1X DPBS and incubated for 24 h in serum-free MEM- α media. The supernatant was collected and centrifuged for 5 min at 400g to remove cell debris before being stored at -80°C until further use.

Part A: Basic MSC characterisation

Growth kinetics

To study the growth kinetics of MSCs, the population doublings (PDs) and population doubling time (PDTs) were calculated by seeding 300 or 3000 cells/cm² (A-MSCs, and BM- and UC-MSCs, respectively) at the start of a passage and counting the number of cells harvested at the end of said passage after reaching 70% confluency. PDTs were calculated as $\text{PDT} = t \times \log_2 / (\log N_t - \log N_0)$, while PDs were calculated as $\text{PD} = \log_2 (N_t / N_0)$; t indicates time in culture, N_t the number of harvested cells and N_0 the number of seeded cells.

Adipogenic and osteogenic differentiation

Adipogenic and osteogenic potential of MSCs was obtained using commercially available media: Adipogenic Differentiation Medium 2 (PromoCell, C-28016) and Osteogenic Differentiation Medium (PromoCell, C-28013), respectively. Harvested MSCs were seeded at a density of 5,700 cells/well for adipogenesis and 2,900 cells/well for osteogenesis in cell culture-treated 96-well plates and kept at 37°C . After 48 h, differentiation was induced by adding differentiation media to positive differentiated cultures while undifferentiated cells were kept in standard growth medium. Medium was replenished twice a week and differentiation assessed after 14 days.

Quantitative analysis of adipogenic and osteogenic differentiation was assessed using the AdipoRedTM Analysis Reagent (Lonza, PT-7009) and OsteoImageTM Mineralization (Lonza, PA-1503), respectively, as per the manufacturer's instructions. For normalisation, cells were also stained with Hoechst 33342 (Invitrogen, Cat-No. 917368). The emitted fluorescent signal from adipogenic and osteogenic quantification and Hoechst staining was measured using a multimode plate reader. Data were presented as a fold-change of the undifferentiated cultures.

Immunophenotypic analysis

Flow cytometry characterisation was performed in each centre according to their routinely used procedures and equipment (Additional file 9: Table S1). MSCs were harvested when cell confluence was reached and resuspended in FACS buffer. Cells were stained at 4°C for 20 min, and data were acquired using conventional flow cytometers. A minimum of 10^4 events was analysed for each marker.

Part B: Functional MSC characterisation

Angiogenic assays

Endothelial cell tube formation assay

Human umbilical cord endothelial vein cells (HUVECs, Lonza, C2519A) were grown in endothelial growth medium (EGM-2, Lonza, CC-3162) until 90% confluent. Further, 48-well plates were coated with 110 μl of growth-factor reduced Matrigel (Corning, 734-1101) and left to gel. HUVECs were harvested and resuspended in MSC-CM at a concentration of 25,000 cells/well. HUVECs stimulated with standard EGM-2 containing 10 ng/ml vascular endothelial growth factor (VEGF) served as positive controls, and cultures with MSC growth medium as negative controls. Plates were then incubated for 18 h, and all conditions were assessed in triplicates. A total of six images were acquired per well with a 4X lens on an Olympus CKX41 brightfield microscope fitted with HD Chrome camera (1/0.8") and 10 \times C-mount adapter and analysed using the angiogenesis analyser plugin for ImageJ (National Institutes of Health, Bethesda, USA).

Wound scratch assay

HUVECs were seeded in 48-well plates at 84,000 cells/cm² and cultured overnight. Subsequently, a p200 tip was used to create a scratch in each monolayer. Cultures were washed with DPBS before adding MSC-CM. Scratches were imaged immediately after the addition of CM (0 h) and after 8 and 24 h incubation using the automated Cytation 1 Imaging Reader at 4X (BioTek, with Gen5 Version 3.04 software, Swindon, UK). Six replicates were undertaken, and the total area of each scratch was measured using Image J and the percentage of closure was calculated relative to time 0 h.

Angiogenesis cytokine array

The relative levels of angiogenesis-related cytokines in the MSC-CM were analysed using the Proteome Profiler Human Cytokine Array Kit from R&D systems (Abingdon, UK, ARY022B) per manufacturer's instructions. Levels of angiogenic cytokines are expressed relative to the internal control of each sample.

Immunomodulatory assays

PBMC proliferation assay

MSC-mediated inhibition of T cell proliferation was assessed as described before [17]. MSCs were seeded one day before adding peripheral blood mononuclear cells (PBMCs) isolated from leukapheresis samples from healthy donors, provided by the German Red Cross Blood Donor Service in Mannheim (Mannheim Ethics Commission; vote number 2018-594N-MA). To assess their proliferation, PBMCs were labelled with proliferation dye Cytotell Green (ATT Bioquest, 22253) (1:500 dilution) and seeded at a 1:10 MSCs:PBMCs ratio in RPMI, supplemented with 10% FBS, 2% L-glutamine (PAN Biotech, P04-80100), 1% Penicillin/Streptomycin (PAN Biotech, P06-07100), and 200 U/ml IL-2 (Promokine, C61240). PBMC proliferation was stimulated with phytohaemagglutinin-L (PHA, 4.8 µg/ml (Biochrom, Merck Millipore, M5030)). PBMCs cultured alone without MSCs in the absence and presence of PHA served as negative and positive controls, respectively.

After 5 days, PBMC proliferation was measured based on the dilution of Cytotell Green dye using a FACS Canto II (BD Biosciences) and the data were analysed with FlowJo Software.

IFN- γ stimulation and intracellular indoleamine 2,3-dioxygenase (IDO) staining

Indoleamine 2,3-dioxygenase (IDO)-mediated tryptophan degradation suppresses T cell proliferation as described before [17]. To assess the level of IDO expression in MSCs, the cells were treated in the presence or absence of interferon γ (IFN- γ 25 ng/ml (R&D Systems, 285-IF) for 24 h. For intracellular IDO staining, MSCs were harvested, fixed, permeabilised and then stained (anti-IDO PE antibody (1:40 dilution) (ThermoFisher Scientific, 12-9477-42)). After washing, the cells' fluorescence was measured with a FACS Canto (BD Biosciences) and the data analysed with FlowJo.

Biodistribution in vivo

Biodistribution of the different MSCs in mice was evaluated by bioluminescence imaging (BLI). For this purpose, the cells were transduced to express a firefly luciferase genetic reporter.

Production of FLuc⁺ expressing cells

MSCs were transduced with a lentiviral vector (LV) encoding the luc2 firefly luciferase (FLuc) reporter. The pHIV-Luc2-ZsGreen vector was a gift from Bryan Welm and Zena Werb (Addgene plasmid #39,196). The LV also contains a gene encoding for a green fluorescent protein, ZsGreen. Lentiviral particles were produced

using standard protocols [18] by co-transfection of HEK cells with the transfer vector (pHIV-Luc2-ZsGreen), an envelope plasmid (pMD2.G) and a packaging plasmid (psPAX2), concentration by ultracentrifugation and titration using HEK cells, based on ZsGreen expression.

To produce the transduced populations, MSCs were infected overnight with a multiplicity of infection of 5 in the presence of 6 µg/mL diethylaminoethyl-dextran (DEAE-dextran) [19]. The cells were then grown until 60–90% confluence before sorting based on ZsGreen fluorescence using a FACSaria II (BD Biosciences) to obtain a pure population of cells expressing the transgene (FLuc⁺ MSCs).

Animal experiments

7–9-week-old C57 Black 6 (C57BL/6) albino female mice were used to evaluate the biodistribution of FLuc⁺ MSCs from their administration into the animal (day 0) up to 7 days later. Mice were obtained from a colony managed by the Biomedical Services Unit at the University of Liverpool (UK). Mice were housed in individually ventilated cages under a 12-h light/dark cycle and provided with standard food and water ad libitum. All animal procedures were performed under a licence granted under the UK's Animals (Scientific Procedures) Act 1986 and were approved by the University of Liverpool Animal Welfare and Ethics Research Board (project title: Developing safe and efficacious cell-based therapies for kidney disease; committee: UK's Home Office; approval number: PP3076489; approval date: 02.11.2020). Our data are reported in line with the ARRIVE guidelines.

FLuc⁺ MSCs were harvested and suspended in ice-cold DPBS at a concentration of 2.5×10^5 cells/100 µL and kept on ice until administration. Animals ($n=4$ per donor per cell type) were anaesthetised with isoflurane and intravenously (IV) injected with 100 µL of cell suspension through the tail vein, followed by subcutaneous administration (SC) of 200 µL of 47 mM D-Luciferin 20 min before imaging [20]. The administration of the substrate and the imaging were performed immediately after the injection of the cells (day 0) and after 1, 3 and 7 days. Data were acquired using an IVIS Spectrum system (Perkin Elmer). The acquired signal was always normalised to radiance (photons/second/centimeter²/steradian) and the signal coming from the thoracic area of the animals was quantified using the region of interest (ROI) tool of the IVIS software (Living Image v. 4.5.2) to obtain the total number of photons emitted in that specific area and displayed as total flux (photons/s). Each imaging session was performed using open filter, binning of 8, f-stop of 1-, and 60-s exposure time at day 0, and 180 s exposure time at days 1, 3 and 7.

Statistical analysis

Quantitative data are reported as mean \pm standard deviation (SD). *N* indicates the number of biological replicates, *n* the number of independent technical replicates. Statistical analyses were performed using GraphPad Prism version 9.2.0 (GraphPad Software, Inc., San Diego, CA, USA). The type of statistical test and the number of replicates included in the analyses are indicated in the figure legends. A *p* value < 0.05 was considered statistically significant.

Results

Cell culture harmonisation

The first steps to guarantee a reliable head-to-head comparison of the three different MSC sources were directed towards the harmonisation of methodologies across centres. Thus, we defined a common protocol to expand MSCs based on three key parameters: an identical basal medium, namely MEM- α , one defined batch of FBS and a defined expansion plating density.

Batch-to-batch variability of FBS is a crucial factor in MSC manufacture [21]. We tested three different sera lots on previously isolated BM-MSCs and selected the lot (FBS-A) which supported cell growth and maintained the MSC phenotype in accordance with the ISCT minimal criteria [22]—namely trilineage differentiation, expression of CD73, CD90 and CD105, and the absence of CD34, CD45, CD11b, CD19, and HLA-DR markers (Additional file 1: Fig. S1).

As plating density can affect proliferation kinetics of MSCs [16, 23], cells from all tissue sources were grown for at least two passages under two seeding densities: 300 and 3000 cells/cm². At higher seeding density, A- and BM-MSCs had lower cumulative population doublings (CPD), leading to a prolongation of their expansion time (Additional file 2: Fig. S2a, c, g). Contrarily, UC-MSCs showed higher CPD when grown at the higher density (Additional file 2: Fig. S2e), indicating decreased PDTs (Additional file 2: Fig. S2g). When assessing cell morphology, UC-MSC lost their spindle-shaped structure when grown at 300 cells/cm² and tended to aggregate and form colonies (Additional file 2: Fig. S2f). A similar effect was observed with BM-MSCs, exhibiting a larger and extended cytoplasm (Additional file 2: Fig. S2d). The opposite was observed for A-MSCs, which showed a

more MSC-like phenotype when grown at 300 cells/cm² (Additional file 2: Fig. S2b). Based on these results, BM- and UC-MSCs were expanded at 3000 cells/cm² while A-MSCs at 300 cells/cm².

Part A: Biological comparison

Having harmonised methodologies, we assessed to which degree they were able to reduce variabilities in a multicentre comparison. BM- and UC-MSCs, each from three different donors, initiated in one laboratory, were shipped as cryopreserved aliquots to the three sites. Using the harmonised culture protocol (identical FBS lot and culture medium and defined seeding densities), cells were cultured at the three centres for three passages to determine their growth kinetics (Fig. 2a, b). The results showed that the trends of growth kinetics were consistent across all the sites, despite each type of MSCs being isolated in different laboratories and shipped internationally. BM-MSCs consistently showed the longest PDT in all sites (90.81 \pm 10.57 h—Heidelberg, 66.78 \pm 16.32 h—Galway, 95.72 \pm 28.02 h—Liverpool) as compared to A-MSCs (43.17 \pm 3.84 h, 37.25 \pm 1.64 h, 51.10 \pm 1.25 h in Heidelberg, Galway and Liverpool, respectively) and UC-MSCs (68.07 \pm 9.11 h, 38.06 \pm 1.04 h, 46.06 \pm 9.47 h in Heidelberg, Galway and Liverpool, respectively) (Fig. 2a). All cells retained their phenotype during culture (Additional file 3: Fig. S3). Despite the harmonised culture conditions, some site-to-site variations in PDT were observed (Fig. 2b), particularly for A- and UC-MSCs where the PDT between sites showed a statistically significant difference. Within all three sites, the PDT varied between donors of the same MSC source and between passages of the same donor (Additional file 4: Fig. S4a-c). These differences between passages could be observed from the wide distribution of PDTs per donor, as the three data points within a single donor represent PDTs from three consecutive passages. A-MSCs showed the least variation across the different sites and donors. UC-MSCs also showed stable growth throughout the three passages, except in Heidelberg where the difference of PDTs across passages was more prominent than in the other sites. Lastly, BM-MSCs consistently showed high donor-to-donor and passage-to-passage differences in all sites.

(See figure on next page.)

Fig. 2 Biological comparison of different tissue sources of MSCs across independent laboratories. **a** In all sites, A- and UC-MSCs showed enhanced growth kinetics when compared to BM-MSCs, with mean doubling times closer to 40 h for A- and UC-, and 80 to 100 h for BM-MSCs. **b** Significant differences were observed between sites when comparing the growth rates between sources. **c, d** A- and BM-MSC were able to undergo different levels of adipogenesis and **e, f** osteogenesis while UC-MSCs showed a limited ability to differentiate only into osteocytes (one out of 3 donors at one site). **g–i** Analysis of the immunophenotype by flow cytometry showed adherence to the minimal criteria in all sites, with higher than 95% expression of CD73, CD90 and CD105. Expression of negative markers showed a moderate increase in CD34 (two sites) and CD45 (one site) in A-MSC preparations and a mild increase in HLA-DR in BM-MSC preparations. Data displayed as mean \pm SD, *N* = 3. **a** One-Way ANOVA with Tukey's multiple comparison corrections, **p* < 0.05, ***p* < 0.001, ****p* < 0.001, *****p* < 0.001.

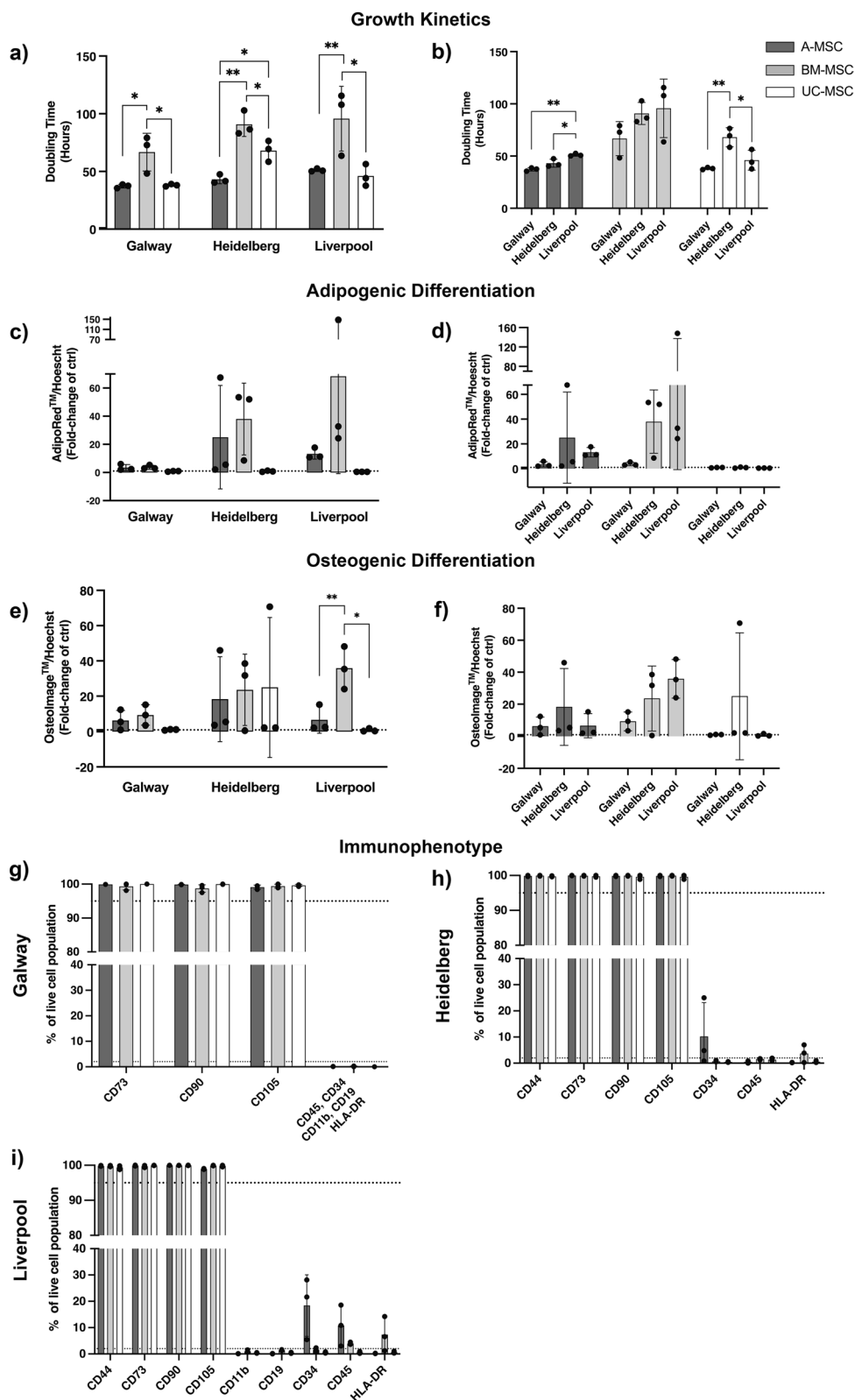


Fig. 2 (See legend on previous page.)

Having established similarities in cell growth, we next assessed the differentiation capacity of the three cell types and between sites (Fig. 2c–f, data depicted as a fold change of the negative control). Despite the use of harmonised protocols, including commercially available reagents, our results demonstrate high levels of variability, mainly related to inter-lab handling, tissue origin, and donor intrinsic factors. A- and BM-MSCs had a greater propensity to differentiate into adipocytes and osteocytes, despite remarkable differences between sites, while UC-MSCs showed negligible levels of differentiation (Fig. 2c–f). BM-MSCs displayed the greatest ability to undergo adipogenesis and osteogenesis, but a high degree of variability was observed when comparing inter-lab data and donor-to-donor results (Additional file 4: Fig. S4d–i). A-MSC showed similar levels of differentiation in all sites, except one donor showing superior induction abilities in Heidelberg. The wide range of differentiation detected in each site: A- and BM- MSCs possessed considerable higher differentiation abilities for both lineages in Liverpool and Heidelberg. Meanwhile in Galway, differentiation of all MSCs remained relatively modest. Furthermore, greater donor-to-donor variability of MSC differentiation from all tissue sources was more prominent in Liverpool and Heidelberg than in Galway (Fig. 2c–f; Additional file 4: Fig. S4d–i; Additional file 5: Fig. S5a–c).

Next, we interrogated the immunophenotype of MSCs using flow cytometry based on the minimal criteria defined previously [22]. Our analysis showed that MSCs from all sources expressed consistently high levels (> 95%) of classical MSC markers CD73, CD90 and CD105 across all sites (Fig. 2g–i). In Heidelberg and Liverpool, A-MSCs expressed rather high levels of negative surface markers such as CD34 ($10.21 \pm 12.96\%$ in Heidelberg and $18.40 \pm 11.69\%$ in Liverpool) and CD45 ($10.81 \pm 7.77\%$ in Liverpool). Noticeable levels of HLA-DR were also observed in BM-MSCs in the Heidelberg and Liverpool sites ($3.70 \pm 3.36\%$ and $7.33 \pm 6.51\%$, respectively), but not in Galway (Additional file 4: Fig. S4j–l).

Part B: Functional in vitro comparison

The characterisation of MSCs coming from different sources using the same culture conditions is relatively unexplored and an important step towards defining

MSCs in any in vitro or in vivo comparative study. To investigate whether and to which extent MSCs of different tissue origins differ, we assessed key functional characteristics together with in vivo behaviour in part B of this study.

Angiogenic and endothelial wound healing properties

Support of angiogenesis and endothelial migration is a relevant mechanism of action of MSC-based therapeutics [12]. The angiogenic properties of CM produced by A-, BM-, and UC-MSCs were assessed in vitro by testing the ability of their secreted factors to induce endothelial cells to form tubule-like structures when seeded in a Matrigel™ substrate. BM-CM significantly enhanced the generation of a larger and more complex network of tubule-like structures than A- and UC-CM (Fig. 3a). BM-CM generated tubular networks with significantly more segments (Fig. 3b), junctions (Fig. 3c), and closed loops (Fig. 3d). Evidence of donor-to-donor variability was observed across all cell sources and was statistically significant different for A-MSC—number of junctions—and BM-MSCs—number of junctions and closed loops— (Additional file 6: Fig. S6a–c). The presence of angiogenic cytokines in MSC-CM was analysed using an antibody array. All sources secreted comparable levels of angiogenic factors; however, differences could be observed in key factors such as VEGF and IGFBP-1 and 2—higher in BM-CM—or IL-8 and MCP-1—higher in UC-CM (Fig. 3e).

The ability of MSC-CM to induce endothelial cell migration was tested in an in vitro wound healing scratch assay. BM-CM resulted in a significant reduction of the scratch gap after 8 and 24 h ($35.03 \pm 6.8\%$ and $58.3 \pm 10.36\%$, respectively) compared to the negative control ($13.73 \pm 1.26\%$ and $3.5 \pm 3.3\%$ at 24 h; Fig. 4). The ability of BM-CM to induce endothelial cell migration was significantly superior to A-CM at 24 h ($22.4 \pm 2.9\%$) and UC-CM at 8 and 24 h ($18.01 \pm 1.7\%$ and $18.1 \pm 6.15\%$, respectively) (Fig. 4a). Limited donor-to-donor variability was observed (Additional file 6: Fig. S6g) although donors with enhanced wound healing properties—such as BM-01 (Additional file 6: Fig. S6g)—also exhibited superior abilities to generate tubule-like structures (Additional file 6: Fig. S6a–c).

(See figure on next page.)

Fig. 3 In vitro angiogenic properties of MSCs. **a** Representative phase contrast images of tubule-like networks in culture. **b–d** BM-CM generated significantly more tubular-like structures in a more complex and extended mesh (**b**), represented by a significantly higher number of junctions (**c**) and closed loops (**d**) than its counterparts in a model of in vitro tubulogenesis. Data expressed as a fold-change of the positive control. **e** Differential angiogenic proteomic profile for each MSC-CM using an antibody array. Data expressed as a fold change of the reference spots. Data displayed as mean \pm SD, $N = 3$, $n = 3$. Two-Way ANOVA with Tukey's multiple comparison corrections, * $p < 0.05$, ** $p < 0.001$, *** $p < 0.0001$, **** $p < 0.00001$.

#Significance relative to negative control

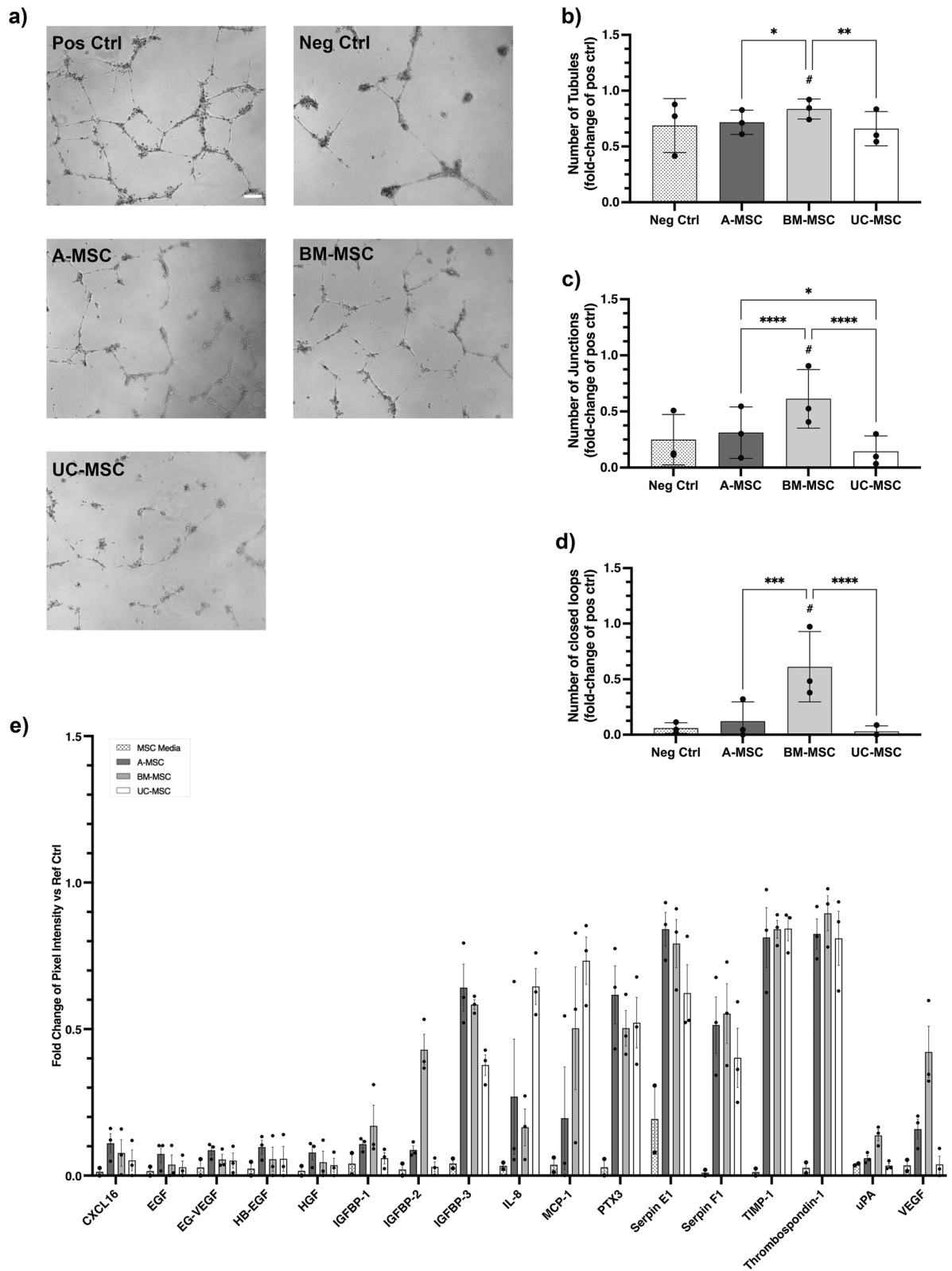


Fig. 3 (See legend on previous page.)

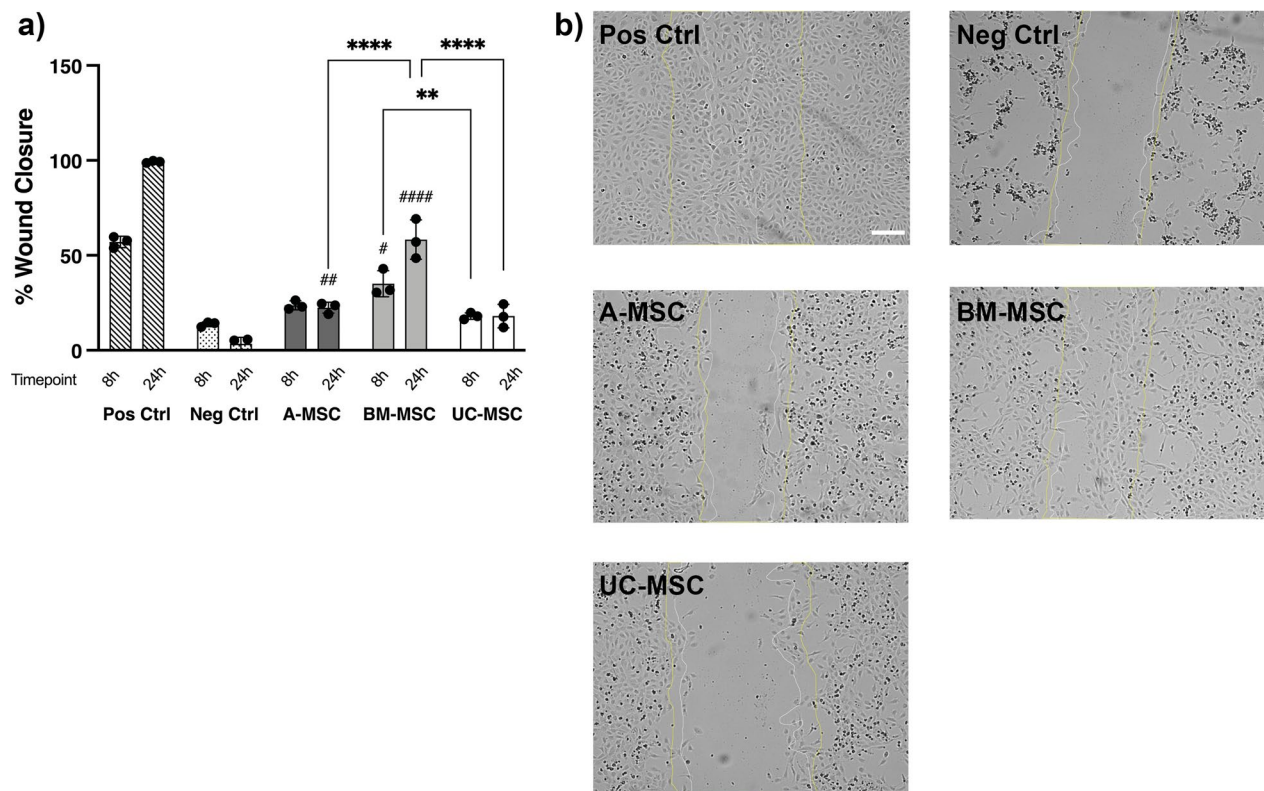


Fig. 4 In vitro wound healing properties of MSCs. **a** BM-CM displayed superior ability to induce endothelial cell migration in an in vitro wound healing model at 8 and 24 h after injury. **b** Representative phase contrast images at time 24 h after scratch; yellow lines show wound width at time 0 h and white lines at time 8 h after scratch. Increased wound gap can be observed at 24 h in the negative control due to cell death, when HUVECs are grown with serum-free MEM- α . Data displayed as mean \pm SD, $N=3$, $n=3$. Two-way ANOVA with Tukey's multiple comparison corrections, * $p < 0.05$, ** $p < 0.001$, *** $p < 0.0001$, **** $p < 0.00001$. #Significance relative to negative control

Immunomodulatory properties

Immunomodulation is a key MSC therapeutic effect [12]. The ability to inhibit PBMC proliferation upon PHA stimulation is often taken as a measure of the immunomodulatory strength [24, 25]. All MSCs were able to suppress PBMC proliferation, as reflected by a decrease in the number of proliferating PBMCs co-cultured with MSCs when compared to those cultured without (Fig. 5a). In the presence of A-MSCs PBMC proliferation was significantly reduced ($17 \pm 5.2\%$ proliferation relative to positive control), followed by BM- ($52 \pm 7\%$) and UC-MSCs ($61 \pm 21\%$).

The ability of MSCs to inhibit PBMC proliferation was compared to their ability to secrete IDO upon IFN- γ stimulation, since the IDO-kynurenine axis has been shown to be responsible for MSC immunomodulation of T-cells [17]. The level of intracellular IDO, indicated by mean fluorescence intensity (MFI) value, was highest in A-MSCs, followed by BM- and UC-MSCs. High donor-to-donor variability was apparent; highest in A-MSC with values ranging from 5294 ± 3752 MFI values (Fig. 5b). The percentage of cells positive for IDO

staining showed the same order, A-MSCs followed by BM- and UC-MSCs; yet here less donor-to-donor variability was observed in all MSC sources ($88.77 \pm 12.04\%$, $76.17 \pm 6.52\%$ and $59.77 \pm 14.15\%$ for A-, BM-, UC-MSCs, respectively; Fig. 5c). Contradicting the notion that IDO levels may correlate with inhibitory strength, donor A-02, the A-MSC donor with the highest ability to suppress PBMC proliferation amongst all A-MSC donors (Additional file 7: Fig. S7a), demonstrated the lowest level of intracellular IDO (Additional file 7: Fig. S7b, c). In contrast, A-01 with the lowest inhibition of PBMC proliferation amongst A-MSC donors exhibited the highest level of intracellular IDO.

In vivo biodistribution in healthy mice

We compared the biodistribution of FLuc⁺ MSCs following their IV administration to healthy C57BL/6J albino mice. Regardless of the MSC type, the BLI images reveal that immediately after administration, all signal originating from the injected cells localised to the thoracic region of the body, corresponding to lungs (Fig. 6a). 24 h after infusion the signal was strongly

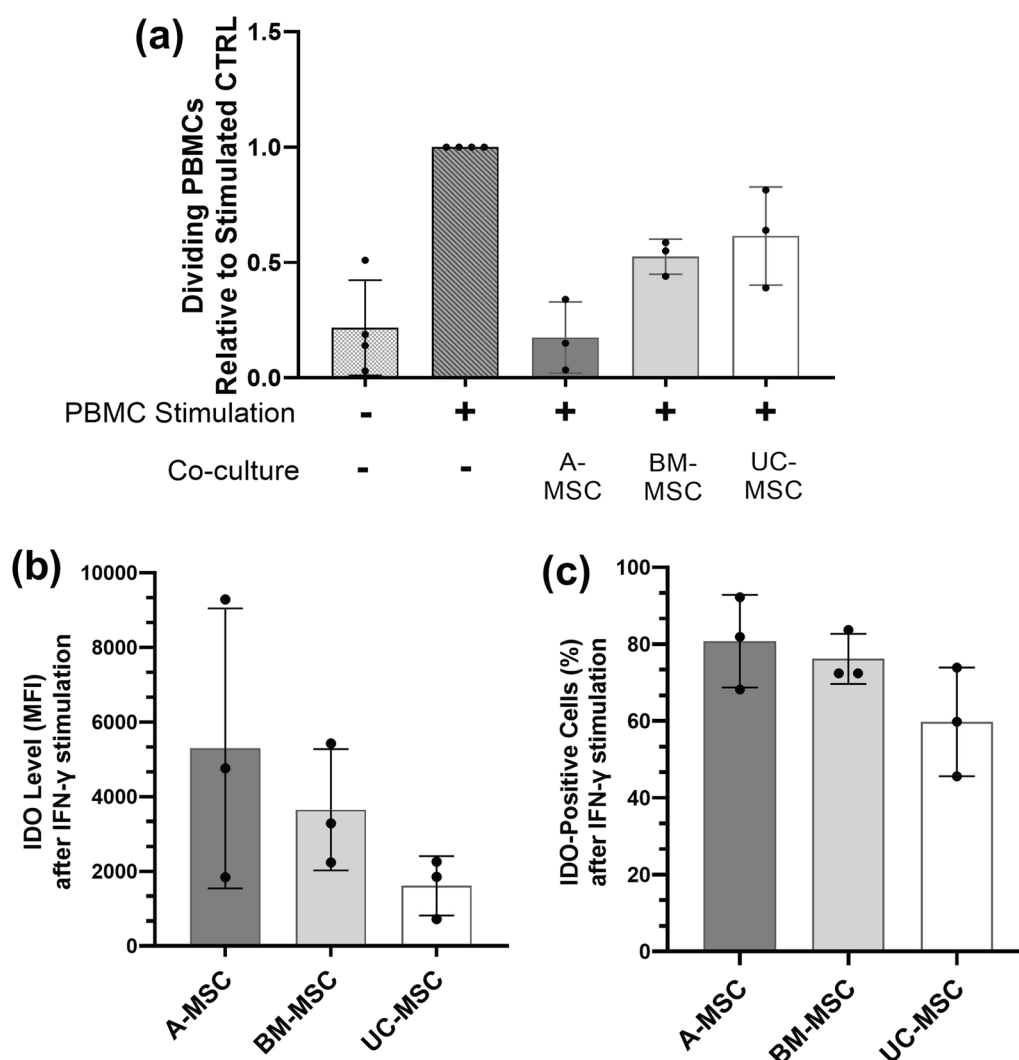


Fig. 5 In vitro immunomodulatory capacities of MSCs. **a** PBMC proliferation after five days co-culture with MSCs under PHA stimulation. All values were normalised to PHA-stimulated monoculture PBMCs. **b** Mean fluorescence intensity of intracellular IDO of MSCs after being treated with IFN- γ for 24 h. **c** The percentage of cells positive for IDO intracellular staining. Data are displayed as mean \pm SD from $N=3$, $n=3$. Two-way ANOVA with Tukey's multiple comparison corrections, * $p < 0.05$

reduced and there was no sign of cell migration from the lungs to any other sites or organs. At this time point, the signal coming from the BM-MSCs seemed weaker than the signal coming from the two other cell types. 3 days after administration a weak signal was detectable from mice that received A- and UC-MSCs, while no signal was detected in most of the mice that received the BM-MSCs. 7 days post-administration there was no detectable bioluminescence in any of the animals (Fig. 6a). These results were confirmed by quantitative analysis of the bioluminescence signal (Fig. 6b and Additional file 8: Fig. S8). The signal obtained at day 0 was comparable not only between the donors of the same cell type (Additional file 8: Fig. S8), but also among

the different sources of cells ($2.8 \times 10^7 \pm 0.99 \times 10^7$ p/s, $4.1 \times 10^7 \pm 0.91 \times 10^7$ p/s and $5.1 \times 10^7 \pm 1.7 \times 10^7$ p/s for A, BM and UC cells, respectively; Fig. 6b). Furthermore, they all showed a similar reduction in the signal from day 0 to day 1 ($3.4 \times 10^6 \pm 0.54 \times 10^6$ p/s, $0.83 \times 10^6 \pm 0.9 \times 10^6$ p/s and $3.6 \times 10^6 \pm 2.5 \times 10^6$ p/s for A, BM and UC cells, respectively) and to day 3 ($8.3 \times 10^5 \pm 2.0 \times 10^5$ p/s, $1.6 \times 10^5 \pm 0.76 \times 10^5$ p/s and $2.9 \times 10^5 \pm 1.1 \times 10^5$ p/s). By day 7 the detected signal ($1.04 \times 10^5 \pm 0.11 \times 10^5$ p/s, $1.07 \times 10^5 \pm 0.26 \times 10^5$ p/s and $0.97 \times 10^5 \pm 0.09 \times 10^5$ p/s, respectively) was no different from the naïve animals ($1.1 \times 10^5 \pm 0.07 \times 10^5$ p/s) that did not receive any cells or substrate. The analysis of relative bioluminescence intensity normalised to

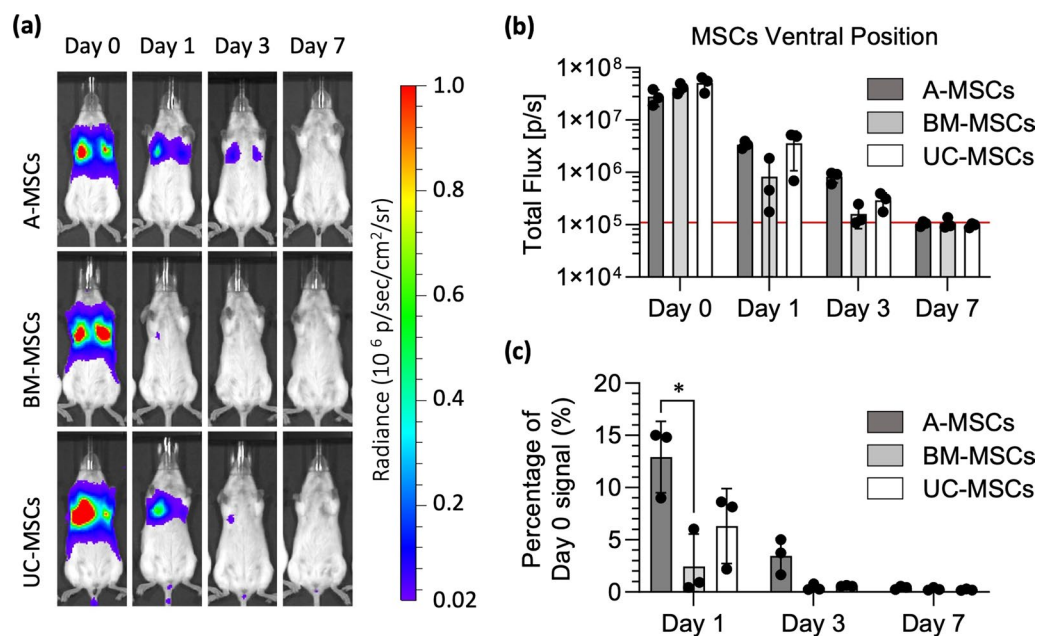


Fig. 6 All MSCs were entrapped in the lungs and were short-lived following IV administration. **a** Representative bioluminescence images of mice administered with FLuc expressing A-, BM- and UC-MSCs on the day of administration of the cells (day 0), and after 1, 3 and 7 days (radiance scale from 0.2×10^5 to 1×10^6 p/s/cm²/sr). **b** Light output (flux) as a function of time (days) from the three different types of MSC. **c** Signal at day 1, day 3, and day 7 normalised to day 0 signal. Data in charts are displayed as mean \pm SD from three donors for each type of MSC (4 animals used per donor). Two-Way ANOVA with Tukey's multiple comparison corrections, * $p < 0.05$

signal at day 0 revealed that in the first 24 h the signal dropped significantly to $12.9 \pm 3.4\%$ for the A-MSCs, to $2.5 \pm 3.1\%$ for the BM cells and to $6.3 \pm 3.6\%$ for the UC cells (Fig. 6c). By day 3, only $3.47 \pm 1.7\%$, $0.44 \pm 0.31\%$ and $0.58 \pm 0.05\%$ of the original signal were detectable for A-, BM- and UC-MSCs, respectively.

Discussion

Within this study, we first aimed to assess the impact of different decentralised production sites on MSC characteristics and second to understand differences in tissue source-specific properties.

Contrary to Stroncek et al., who shipped the same tissue starting material to the different manufacturing sites [26], we mimicked the situation of one initial manufacturing centre and different decentralised cell production facilities that expand MSCs using harmonised protocols and quality control the final MSC product. We pre-defined harmonised conditions by culturing all three MSC types in the same MEM- α supplemented with the same lot of FBS. Finally, to properly compare the different sources, a seeding density optimal for the expansion of each cell type was identified and adopted across centres.

In part A, our study shows for the first time that the protocol harmonisation reduces but not eliminates site-to-site variation whilst the tissue and donor-specific differences remain apparent. BM-MSCs exhibited

the longest doubling time as well as the highest inter-donor variability, whereas A-MSCs consistently showed the least donor-to-donor variation regardless of where they were cultured. Site-to-site variation can in part be attributed to the differing shipment duration on dry ice, which interrupted the cold chain. The manual handling of cell counting and assessment of confluence for harvest also contributed to the site-to-site variations. Given that MSCs show contact-dependent growth inhibition [23], slight differences in the confluence may affect the calculation of growth kinetics. More objectified, operator-independent, assessment of confluence and cell counting is expected to significantly improve comparability.

The analysis of adipogenic and osteogenic potential confirmed the known inter-donor variability that was consistent in all sites. Despite the use of harmonised differentiation protocols and kits, quantitative results varied largely, demonstrating the large influence exerted by the operator. UC cells displayed no adipogenic or osteogenic potential in any of the centres. Reduced or entire lack of adipogenic differentiation potential has been repeatedly reported for perinatal MSCs [27, 28]. Yet, the entire lack of in vitro osteogenic differentiation in UC-MSCs (with one most probably artefactual outlier in one site) was rather unexpected. It may reflect differing requirements of UC-MSCs for osteoinduction [29]. However, it is not

clear whether the in vitro differentiation potential is a meaningful selection criterion when defining the best source of MSC for the intended therapeutic application [4, 10]. We suggest that if differentiation potential is taken as critical attribute, it should be assessed qualitatively, or if quantitatively, as a batch comparison within one centre.

Expression of surface markers (including CD73, CD90 and CD105) and lack of hematopoietic markers (including CD11b, CD19, CD34 and CD45) and major histocompatibility complex (MHC) class II (HLA-DR) are widely accepted criteria to assess the identity and purity of MSCs [22]. Whilst in the three centres MSCs from all donors showed a positivity of at least 98% for all the positive markers, some variability was observed for the negative ones. In particular, A-MSCs showed increased expression (>2%) of CD34 (Heidelberg and Liverpool) and CD45 (Liverpool). Although differences in antigen detection can be due to variable levels of affinity when using different monoclonal antibodies, previous studies have reported CD34 positivity of A-MSCs early in culture [30–32]. Similar early expression of CD45 disappearing after prolonged culture was also observed in BM-MSCs [33]. Moreover, 2 of the 3 BM-MSCs showed a small variability in the positivity to HLA-DR in two centres (Heidelberg and Liverpool). Similar findings have been previously reported by Grau-Vorster et al. who revealed variability in BM-MSC preparations for clinical applications, concluding that the absence or presence of HLA-DR does not have an impact on the overall properties of the cells [34]. Of note, CD34 and HLA-DR positivity observed in the two separate sites in the same donors strongly suggest donor-related variability as the main cause.

It is noteworthy that in this study, the cells were isolated in one specific centre, cryopreserved, and then shipped in dry ice before being expanded and compared in each site in parallel. Cryopreservation not only affects the proliferation of the cells [35], but also impacts the differentiation potential [36] and the immunosuppressive properties [37]. However, it has been described to be a transient effect due to the heat-shock stress induced by the thawing process, with functionality being restored after a certain culture period [38]. In this study, the effect of international shipping has not been evaluated in detail. Our data and that of Stroncek, however, clearly suggest that before such a study, cultivation and quality control protocols require not only harmonisation but rather standardisation to minimise site-specific influences as much as possible.

To determine whether the heterogeneity of MSCs from different origins is also reflected in their potential therapeutic abilities, part B of our study provided a comparison of the tissue sources on top of basic cell characteristic assessments. This comparison was performed each in a

single expert centre. First, we assessed the angiogenic profile of CM obtained from A-, BM- and UC-MSCs. In our hands, CM from BM-MSCs showed superior abilities to form tubule-like structures and induce endothelial cell migration in vitro. The overall presence and concentration of angiogenic factors within the CM were found to be superior in BM preparations with increased relative levels of tubulogenesis-driving factors such as VEGF [39, 40]. Although our results align with previous studies showing superior proangiogenic abilities [41] and higher secretion of VEGF in BM-MSC cultures [42], others have conversely reported higher tube formation and angiogenic bioactivity in the secretome of A-MSCs [43, 44]. Most likely, technical discrepancies along with donor-to-donor variability are playing key roles. For instance, dose-dependent levels of VEGF from BM-MSC secretomes have been correlated with angiogenic activity and proposed as a surrogate potency assay for clinical preparations [45]. Donor variability is a well-known phenomenon we have also observed within our sample preparations, emphasising the need to dissect donor characteristics and variability in autologous and allogeneic settings to achieve favourable clinical outcomes [46].

Second, we investigated whether the source of MSCs might influence their immunomodulatory capacity to suppress PBMC proliferation. We also measured IDO production after IFN- γ stimulation as IDO has been implicated as the key factor responsible for inhibition of PBMC proliferation by catabolism of tryptophan to kynurenine [17, 47]. A-MSCs, the tissue source of MSCs with the highest ability to inhibit PBMC proliferation, exhibit the highest level of intracellular IDO upon IFN- γ stimulation, followed by BM and UC-MSCs. Our data however question a correlation between IDO levels and proliferation inhibitory strength, given that the donor which showed the highest inhibition exhibited the least intracellular IDO and vice versa. Although we previously showed that MSC-expressed IDO is key to inhibit PHA-driven T cell proliferation [17], this is most likely not the only factor involved, especially when considering the much more complex situation in vivo. A study by Chinadurai et al. elegantly showed that MSCs can inhibit PBMC proliferation through PD1/PD-L1 [48].

Our data demonstrate that the different MSC types have individual properties, which may have benefits in specific therapeutic settings. A-MSC shows enhanced immunoregulatory abilities, BM-MSC superior angiogenic and wound healing properties, while UC-MSC appears to be the least potent of all three sources. In this sense, whether the assays proposed are able to capture all the properties and attributes from each tissue source needs further validation in specific in vitro and in vivo injury models to confirm their ability to predict therapeutic potency. A more

detailed and complex picture of their secretome, including the shedding of extracellular vesicles [49] and microRNAs [50], the mitochondrial and metabolic properties [51], together with other aspects of their immunomodulatory properties not addressed in this study, might highlight further attributes aligned with desirable clinical outcomes.

Third, an important aspect of this study was to investigate and compare the fate of different MSCs *in vivo* after being cultured using the same manufacturing procedures. Intravenous administration of MSCs is the most common delivery route used in clinical trials [52]. However, it is well known that MSCs get entrapped in the lung, the so-called pulmonary first pass effect [53–55]. Besides posing a risk for embolisation, pulmonary trap reduces the number of cells that could eventually home and engraft to the injured tissue [56]. Here, BLI performed immediately after the IV administration of different MSCs in healthy mice confirmed their entrapment in the lungs, irrespective of their tissue of origin. Additionally, none of the cells escaped the lungs, neither on the day of administration nor in any of the following days. In fact, a major drop in the bioluminescence signal coming from the lungs was observed in the first 24 h post-injection. Despite signal from A-MSCs being still noticeable 3 days post-administration, no signal from any of the MSCs was detected 7 days after injection. This result is consistent with various reports [54, 55] and confirms that this effect is not influenced by MSC origin. When cell therapies are considered, the fact that most of MSCs die in the first 24 h is not necessarily a bad result. It has been proposed that the apoptosis of IV administered MSCs in the lungs and the subsequent phagocytosis of the cell debris by local macrophages is a mechanism of MSC-mediated immunomodulation [55, 57–59].

In summary, we have:

- Provided a harmonised manufacturing workflow that has demonstrated reproducible results across three independent laboratories when expanding MSCs.
- Defined a multi-assay matrix capable of identifying functional differences in terms of angiogenesis, wound healing abilities and immunosuppressive properties.
- Demonstrated similar *in vivo* biodistribution properties regardless of cell origin.

Conclusions

Lack of standard culture protocols is a major limitation that hinders comparison of the clinical benefits of MSCs, especially when they are from different sources,

and produced in different centres. Here we established, for the first time, harmonised tissue culture conditions for expansion of A-, BM- and UC- MSCs among three independent centres across Europe to investigate the reproducibility of these procedures and its impact on their biological characteristics and functionality both *in vitro* and *in vivo*. We show that harmonised protocols improve reproducibility across different centres emphasising the need for worldwide standards to manufacture MSCs for clinical use. Further, tissue-specific differences in cell characteristics suggest a need for selecting the optimal cell type for the intended clinical indication based on source availability and functional characteristics. These results show the heterogeneous behaviour and therapeutic properties of MSCs as a reflection of tissue-origin properties while providing evidence that the use of harmonised culture procedures can reduce but not eliminate inter-lab and operator differences.

Abbreviations

A	Adipose
BLI	Bioluminescence imaging
BM	Bone marrow
CM	Conditioned media
CPD	Cumulative population doublings
DEAE-dextran	Diethylaminoethyl-dextran
DMSO	Dimethyl sulfoxide
DPBS	Dulbecco's phosphate-buffered saline
EGM	Endothelial growth medium
EU	European Union
FACSS	Fluorescence activated cell sorting
FBS	Foetal bovine serum
HEK	Human embryonic kidney cells
HLA-DR	Human leukocyte antigen—DR isotype
HUVEC	Human umbilical cord endothelial vein cells
IDO	Indoleamine 2,3-dioxygenase
IFN- γ	Interferon gamma
IGFBP	Insulin-like growth factor binding protein
IL	Interleukin
ISCT	International society for cell and gene therapy
ITN	Innovative training network
IV	Intravenously
LV	Lentiviral vector
MCP-1	Monocyte chemoattractant protein 1
MEM- α	Minimum essential medium alpha
MFI	Mean fluorescence intensity
MHC	Major histocompatibility complex
MOI	Multiplicity of infection
MSC	Mesenchymal stromal cell
PBMC	Peripheral blood mononuclear cells
PD	Population doublings
PDT	Population doubling time
PHA	Phytohemagglutinin-L
ROI	Region of interest
RPMI	Roswell Park Memorial Institute Medium
SC	Subcutaneous
SD	Standard deviation
UC	Umbilical cord
VEGF	Vascular endothelial growth factor

Supplementary Information

The online version contains supplementary material available at <https://doi.org/10.1186/s13287-023-03352-1>.

Additional file 1: Supplementary Fig. S1. Cell Culture Harmonisation: Serum Screen. Population doubling times and phase contrast images of three BM-MSCs donors showed that exclusively FBS A supported cell growth and fibroblast-like morphology. Therefore, further experiments were carried out using serum A. Flow cytometry confirmed the expression of positive surface antigens and lack of negative markers in two out of three populations grown with FBS A. BM-MSC cultures were induced to differentiate into adipocytes while undifferentiated cultures served as control. Images of Oil Red O are shown in panel and quantification of Oil Red O stain retention in panel. Both show an increase in lipid content in the majority of adipogenic differentiated cultures. Osteogenic differentiated cultures showed presence of calcium in the extracellular matrix with Alizarin Red staining. Quantification of extracted calcium from osteogenically differentiated BM-MSC showed more than 1 µg of calcium per well in all differentiated cultures. Quantification of sulphated glycosaminoglycans showed significantly increased levels in differentiated cultures, confirming their mesodermal differentiation abilities. Data displayed as mean ± SD, N=3. Two-Way ANOVA with Bonferroni's multiple comparison corrections, * = p < 0.05, ** = p < 0.001, *** = p < 0.0001, **** = p < 0.00001. Pictures taken at 40X; scale bar 500 µm.

Additional file 2: Supplementary Fig. S2. Cell Culture Harmonisation: Seeding Density. Comparison between seeding density confirmed differences in cell source. Cumulative population doublings were calculated by culturing MSCs at 300 and 3,000 cells/cm² in all three different sites. A-MSC and BM-MSC showed a rapid increase in cumulative doublings when seeded at a lower density versus at high density after the same period in culture. UC-MSC conversely had increased cumulative doublings when seeded at higher density. When comparing population doubling times, A-MSC and BM-MSC had prolonged kinetics when grown at 3,000 cells/cm² whereas UC-MSC divided faster at 3,000 cells/cm². Representative phase contrast images of MSCs. Data displayed as mean ± SD, N=3. Pictures taken at 40X.

Additional file 3: Supplementary Fig. S3. Representative phase contrast images of MSCs in all sites at early and latest stages of culture. Pictures taken at 100X; scale bar 200 µm.

Additional file 4: Supplementary Fig. S4. Biological comparison: donor-by-donor breakdown of doubling times, immunophenotype, differentiation results and phase contrast images of the differentiation. Figures show the individual doubling times per each donor in all sites. The three dots within a single donor represent the doubling times from three consecutive passages. Across laboratories, A- and UC- showed stable proliferation rates when looking at individual donors. Greater differences were seen in BM- in terms of donor-to-donor variability, although each donor behaved similarly regardless of manufacturing site. In terms of committing to mesodermal lineages, high variability of induction was seen across laboratories. Broadly, A- and BM- donors were able to undergo adipogenesis in two sites, apart from one particular donor that showed induction in all laboratories. Negligible levels of adipogenic differentiation were seen in UC-MSC cultures. Similarly, A- and BM-MSCs were able to undergo osteogenic differentiation in two out of three sites, albeit not all donors and at remarkable different rates; exclusively one UC-MSCs in one site showed moderate levels of osteogenesis. Assessment of surface antigen expression confirmed >95% levels of CD73, CD90 and CD105 in all donors across sites. However, two preparations of A-MSC showed higher than 2% levels of CD34 in two and CD45 in one site. Importantly, these were the same donors. Data displayed as mean ± SD, N=3, n=3. One-Way ANOVA with Tukey's multiple comparison corrections, * = p < 0.05, ** = p < 0.001, *** = p < 0.0001, **** = p < 0.00001.

Additional file 5: Supplementary Fig. S5. Representative phase contrast images of MSC at the end of the adipogenic and osteogenic differentiation procedure in comparison with undifferentiated cultures in each site. Pictures taken at 100X; scale bar 200 µm.

Additional file 6: Supplementary Fig. S6. Angiogenic and wound healing properties of MSCs listed by donor. Number of tubules, junctions and closed loops generated by each donor. Data expressed as a fold-change of the positive control; mean ± SD, n = 3. Differential angiogenic proteomic profile detected for A-, BM- and UC-MSCs. Data expressed as fold change of the internal reference spots. Wound closure induced by each donor per cell source at 8 and 24 hours. Data displayed as mean ± SD, n = 3. Two-Way ANOVA with Tukey's multiple comparison corrections, * = p < 0.05, ** = p < 0.001, *** = p < 0.0001, **** = p < 0.00001. # Significance relative to negative control.

Additional file 7: Supplementary Fig. S7. Donor-by-donor breakdown of MSC immunomodulatory capacity. Individual values of PBMC proliferation co-cultured with MSCs in the presence of PHA, where each bar represents the relative value in relation to PHA-stimulated PBMCs cultured alone. MFI of IDO intracellular staining and percentage of IDO-positive cells after 24h of IFN-γ stimulation, listed per donor.

Additional file 8: Supplementary Fig. S8. Donor-by-donor breakdown of the signal obtained from the in vivo imaging of MSCs in healthy C57BL/6 albino mice. Light output as a function of time coming from A-, BM-, and UC-MSCs. Data displayed as mean ± SD from N = 4 for each donor. The red line is the background BLI signal emitted by naïve animal that did not receive any cells.

Additional file 9: Supplementary Table S1. Detailed methodology used in each centre to characterise the immunophenotype of MSCs.

Acknowledgements

The team in Galway would like to acknowledge technical and consultative support for flow cytometry experiments provided by Dr. Shirley Hanley of the University of Galway Flow Cytometry Core Facility, which is supported by funds from University of Galway, Science Foundation Ireland, the Irish Government's Programme for Research in Third Level Institutions, Cycle 5 and the European Regional Development Fund. The team in Mannheim acknowledges the excellent support of Stefanie Uhlig, FlowCore Mannheim and Institute of Transfusion Medicine and Immunology, and Corinna Thielemann for excellent technical support. The team in Liverpool acknowledges the support of the Flow Cytometry Facility.

Author contributions

All authors were major contributors in the conception and design of the study, read and approved the final manuscript. SCiC, ER, ES, FA acquired, analysed and interpreted the data and drafted and revised the manuscript. PM, TB, KB provided financial support. VH, BW, AT provided material and specific methodological expertise to the study. All authors read and approved the final manuscript.

Funding

Open Access funding enabled and organized by Projekt DEAL, we specifically acknowledge financial support by Deutsche Forschungsgemeinschaft within the funding programme "Open Access Publikationskosten" as well as by Heidelberg University. This project has received funding from the European Union's Horizon 2020 research and innovation programme under the Marie Skłodowska-Curie grant agreement No 813839.

Availability of data and materials

The datasets used and/or analysed during the current study are available from the corresponding author on reasonable request.

Declarations

Ethics approval

A-MSCs from lipoaspirates (healthy donors of both gender in a range of age 47–25 years) were processed in Heidelberg after obtaining informed consent (Mannheim Ethics Commission; vote number 2006-192NMA). BM-MSCs provided by Galway were isolated from bone marrow aspirates (healthy young male donors) purchased from Lonza (Basel, Switzerland), and UC-MSCs with

informed consent obtained in accordance with the Declaration of Helsinki were sourced from the NHS Blood and Transplant and transferred to the University of Liverpool. All animal procedures were performed under a licence granted under the UK's Animals (Scientific Procedures) Act 1986 and were approved by the University of Liverpool Animal Welfare and Ethics Research Board.

Consent for publication

Not applicable.

Competing interests

The authors declare that they have no competing interests. Timothy O'Brien, co-author of this manuscript and Editor-in-Chief of *Stem Cell Research & Therapy*, declares that he was not involved in the peer review or decision making of this article.

Author details

¹College of Medicine, Nursing and Health Science, School of Medicine, Regenerative Medicine Institute (REMEDI), University of Galway, Galway, Ireland. ²Institute of Transfusion Medicine and Immunology, Medical Faculty Mannheim, Heidelberg University, German Red Cross Blood Service, Baden-Württemberg-Hessen, Friedrich-Ebert Str. 107, 68167 Mannheim, Germany. ³Department of Molecular Physiology and Cell Signalling, University of Liverpool, Liverpool, UK. ⁴Cellular Therapies Laboratory, NHS Blood and Transplant, Liverpool, UK. ⁵Centre for Preclinical Imaging, University of Liverpool, Liverpool, UK. ⁶CURAM, SFI Research Centre for Medical Devices, University of Galway, Galway, Ireland. ⁷Mannheim Institute of Innate Immunoscience, Medical Faculty Mannheim, Heidelberg University, Mannheim, Germany.

Received: 30 November 2022 Accepted: 20 April 2023

Published online: 04 May 2023

References

- Pittenger MF, Discher DE, Peault BM, Phinney DG, Hare JM, Caplan AI. Mesenchymal stem cell perspective: cell biology to clinical progress. *NPJ Regen Med.* 2019;4:22.
- Prockop DJ. The exciting prospects of new therapies with mesenchymal stromal cells. *Cytotherapy.* 2017;19(1):1–8.
- Petrenko Y, Vackova I, Kekulova K, Chudickova M, Koci Z, Turnovcova K, et al. A comparative analysis of multipotent mesenchymal stromal cells derived from different sources, with a focus on neuroregenerative potential. *Sci Rep.* 2020;10(1):4290.
- Calcat ICS, Sanz-Nogues C, O'Brien T. When origin matters: properties of mesenchymal stromal cells from different sources for clinical translation in kidney disease. *Front Med (Lausanne).* 2021;8:728496.
- Galipeau J, Sensebe L. Mesenchymal stromal cells: clinical challenges and therapeutic opportunities. *Cell Stem Cell.* 2018;22(6):824–33.
- Friedenstein AJ, Petrakova KV, Kurolova AI, Frolova GP. Heterotopic of bone marrow. Analysis of precursor cells for osteogenic and hematopoietic tissues. *Transplantation.* 1968;6(2):230–47.
- Rodriguez-Fuentes DE, Fernandez-Garza LE, Samia-Meza JA, Barrera-Barrera SA, Caplan AI, Barrera-Saldana HA. Mesenchymal stem cells current clinical applications: a systematic review. *Arch Med Res.* 2021;52(1):93–101.
- Selich A, Zimmermann K, Tenspolde M, Dittrich-Breiholz O, von Kaisenberg C, Schambach A, et al. Umbilical cord as a long-term source of activatable mesenchymal stromal cells for immunomodulation. *Stem Cell Res Ther.* 2019;10(1):285.
- Amadeo F, Trivino Cepeda K, Littlewood J, Wilm B, Taylor A, Murray P. Mesenchymal stromal cells: what have we learned so far about their therapeutic potential and mechanisms of action? *Emerg Top Life Sci.* 2021;5(4):549–62.
- Wilson AJ, Rand E, Webster AJ, Genever PG. Characterisation of mesenchymal stromal cells in clinical trial reports: analysis of published descriptors. *Stem Cell Res Ther.* 2021;12(1):360.
- Stroncek DF, Jin P, McKenna DH, Takahashi M, Fontaine MJ, Pati S, et al. Human mesenchymal stromal cell (MSC) characteristics vary among laboratories when manufactured from the same source material: a report by the cellular therapy team of the biomedical excellence for safer transfusion (BEST) collaborative. *Front Cell Dev Biol.* 2020;8:458.
- Bieback K, Kuci S, Schafer R. Production and quality testing of multipotent mesenchymal stromal cell therapeutics for clinical use. *Transfusion.* 2019;59(6):2164–73.
- Fontaine MJ, Shih H, Schafer R, Pittenger MF. Unraveling the mesenchymal stromal cells' paracrine immunomodulatory effects. *Transfus Med Rev.* 2016;30(1):37–43.
- Baraniak PR, McDevitt TC. Stem cell paracrine actions and tissue regeneration. *Regen Med.* 2010;5(1):121–43.
- Mohamed SA, Howard L, McInerney V, Hayat A, Krawczyk J, Naughton S, et al. Autologous bone marrow mesenchymal stromal cell therapy for "no-option" critical limb ischemia is limited by karyotype abnormalities. *Cytotherapy.* 2020;22(6):313–21.
- Kern S, Eichler H, Stoeve J, Kluter H, Bieback K. Comparative analysis of mesenchymal stem cells from bone marrow, umbilical cord blood, or adipose tissue. *Stem Cells.* 2006;24(5):1294–301.
- Torres Crigna A, Uhlig S, Elvers-Hornung S, Kluter H, Bieback K. Human Adipose tissue-derived stromal cells suppress human, but not murine lymphocyte proliferation, via indoleamine 2,3-dioxygenase activity. *Cells.* 2020;9(11):2419.
- Kutner RH, Zhang XY, Reiser J. Production, concentration and titration of pseudotyped HIV-1-based lentiviral vectors. *Nat Protoc.* 2009;4(4):495–505.
- Amadeo F, Hanson V, Murray P, Taylor A. DEAE-dextran enhances the lentiviral transduction of primary human mesenchymal stromal cells from all major tissue sources without affecting their proliferation and phenotype. *Mol Biotechnol.* 2022;65(4):544–55.
- Amadeo F, Plagge A, Chacko A, Wilm B, Hanson V, Liptrott N, et al. Firefly luciferase offers superior performance to AkaLuc for tracking the fate of administered cell therapies. *Eur J Nucl Med Mol Imaging.* 2022;49(3):796–808.
- Zheng X, Baker H, Hancock WS, Fawaz F, McCaman M, Pungor E Jr. Proteomic analysis for the assessment of different lots of fetal bovine serum as a raw material for cell culture. Part IV. Application of proteomics to the manufacture of biological drugs. *Biotechnol Prog.* 2006;22(5):1294–300.
- Dominici M, Le Blanc K, Mueller I, Slaper-Cortenbach I, Marini F, Krause D, et al. Minimal criteria for defining multipotent mesenchymal stromal cells. The international society for cellular therapy position statement. *Cytotherapy.* 2006;8(4):315–7.
- Higuera G, Schop D, Janssen F, van Dijkhuizen-Radersma R, van Bostel T, van Blitterswijk CA. Quantifying in vitro growth and metabolism kinetics of human mesenchymal stem cells using a mathematical model. *Tissue Eng Part A.* 2009;15(9):2653–63.
- Le Blanc K, Tammik L, Sundberg B, Haynesworth SE, Ringden O. Mesenchymal stem cells inhibit and stimulate mixed lymphocyte cultures and mitogenic responses independently of the major histocompatibility complex. *Scand J Immunol.* 2003;57(1):11–20.
- Ketterl N, Brachtl G, Schuh C, Bieback K, Schallmoser K, Reinisch A, et al. A robust potency assay highlights significant donor variation of human mesenchymal stem/progenitor cell immune modulatory capacity and extended radio-resistance. *Stem Cell Res Ther.* 2015;6:236.
- Liu S, de Castro LF, Jin P, Civini S, Ren J, Reems JA, et al. Manufacturing differences affect human bone marrow stromal cell characteristics and function: comparison of production methods and products from multiple centers. *Sci Rep.* 2017;7:46731.
- Karagianni M, Brinkmann I, Kinzebach S, Grassl M, Weiss C, Bugert P, et al. A comparative analysis of the adipogenic potential in human mesenchymal stromal cells from cord blood and other sources. *Cytotherapy.* 2013;15(1):76–88.
- Rebelatto CK, Aguiar AM, Moretao MP, Senegaglia AC, Hansen P, Barchiki F, et al. Dissimilar differentiation of mesenchymal stem cells from bone marrow, umbilical cord blood, and adipose tissue. *Exp Biol Med (Maywood).* 2008;233(7):901–13.
- Majore I, Moretti P, Stahl F, Hass R, Kasper C. Growth and differentiation properties of mesenchymal stromal cell populations derived from whole human umbilical cord. *Stem Cell Rev Rep.* 2011;7(1):17–31.
- Quirici N, Scavullo C, de Girolamo L, Lopa S, Arrigoni E, Delilieri GL, et al. Anti-L-NGFR and -CD34 monoclonal antibodies identify multipotent

- mesenchymal stem cells in human adipose tissue. *Stem Cells Dev.* 2010;19(6):915–25.
31. Bourin P, Bunnell BA, Casteilla L, Dominici M, Katz AJ, March KL, et al. Stromal cells from the adipose tissue-derived stromal vascular fraction and culture expanded adipose tissue-derived stromal/stem cells: a joint statement of the International Federation for Adipose Therapeutics and Science (IFATS) and the International Society for Cellular Therapy (ISCT). *Cytotherapy.* 2013;15(6):641–8.
 32. Lin CS, Ning H, Lin G, Lue TF. Is CD34 truly a negative marker for mesenchymal stromal cells? *Cytotherapy.* 2012;14(10):1159–63.
 33. Yeh SP, Chang JG, Lin CL, Lo WJ, Lee CC, Lin CY, et al. Mesenchymal stem cells can be easily isolated from bone marrow of patients with various haematological malignancies but the surface antigens expression may be changed after prolonged ex vivo culture. *Leukemia.* 2005;19(8):1505–7.
 34. Grau-Vorster M, Laitinen A, Nystedt J, Vives J. HLA-DR expression in clinical-grade bone marrow-derived multipotent mesenchymal stromal cells: a two-site study. *Stem Cell Res Ther.* 2019;10(1):164.
 35. Al-Saqi SH, Saliem M, Quezada HC, Ekblad A, Jonasson AF, Hovatta O, et al. Defined serum- and xeno-free cryopreservation of mesenchymal stem cells. *Cell Tissue Bank.* 2015;16(2):181–93.
 36. Bahsoun S, Coopman K, Akam EC. Quantitative assessment of the impact of cryopreservation on human bone marrow-derived mesenchymal stem cells: up to 24 h post-thaw and beyond. *Stem Cell Res Ther.* 2020;11(1):540.
 37. Francois M, Copland IB, Yuan S, Romieu-Mourez R, Waller EK, Galipeau J. Cryopreserved mesenchymal stromal cells display impaired immunosuppressive properties as a result of heat-shock response and impaired interferon-gamma licensing. *Cytotherapy.* 2012;14(2):147–52.
 38. Marquez-Curtis LA, Janowska-Wieczorek A, McGann LE, Elliott JA. Mesenchymal stromal cells derived from various tissues: Biological, clinical and cryopreservation aspects. *Cryobiology.* 2015;71(2):181–97.
 39. Maacha S, Sidahmed H, Jacob S, Gentilcore G, Calzone R, Grivel JC, et al. Paracrine mechanisms of mesenchymal stromal cells in angiogenesis. *Stem Cells Int.* 2020;2020:4356359.
 40. Lehman N, Cutrone R, Raber A, Perry R, Van't Hof W, Deans R, et al. Development of a surrogate angiogenic potency assay for clinical-grade stem cell production. *Cytotherapy.* 2012;14(8):994–1004.
 41. Du WJ, Chi Y, Yang ZX, Li ZJ, Cui JJ, Song BQ, et al. Heterogeneity of proangiogenic features in mesenchymal stem cells derived from bone marrow, adipose tissue, umbilical cord, and placenta. *Stem Cell Res Ther.* 2016;7(1):163.
 42. Peng L, Jia Z, Yin X, Zhang X, Liu Y, Chen P, et al. Comparative analysis of mesenchymal stem cells from bone marrow, cartilage, and adipose tissue. *Stem Cells Dev.* 2008;17(4):761–73.
 43. Hsiao ST, Asgari A, Lokmic Z, Sinclair R, Dusting GJ, Lim SY, et al. Comparative analysis of paracrine factor expression in human adult mesenchymal stem cells derived from bone marrow, adipose, and dermal tissue. *Stem Cells Dev.* 2012;21(12):2189–203.
 44. Kim Y, Kim H, Cho H, Bae Y, Suh K, Jung J. Direct comparison of human mesenchymal stem cells derived from adipose tissues and bone marrow in mediating neovascularization in response to vascular ischemia. *Cell Physiol Biochem.* 2007;20(6):867–76.
 45. Thej C, Ramadas B, Walvekar A, Majumdar AS, Balasubramanian S. Development of a surrogate potency assay to determine the angiogenic activity of Stempeucel(R), a pooled, ex-vivo expanded, allogeneic human bone marrow mesenchymal stromal cell product. *Stem Cell Res Ther.* 2017;8(1):47.
 46. Mastrolia I, Foppiani EM, Murgia A, Candini O, Samarelli AV, Grisendi G, et al. Challenges in clinical development of mesenchymal stromal/stem cells: concise review. *Stem Cells Transl Med.* 2019;8(11):1135–48.
 47. Fiori A, Uhlig S, Kluter H, Bieback K. Human adipose tissue-derived mesenchymal stromal cells inhibit CD4+ T cell proliferation and induce regulatory T cells as well as CD127 expression on CD4+CD25+ T cells. *Cells.* 2021;10(1).
 48. Chinnadurai R, Copland IB, Patel SR, Galipeau J. IDO-independent suppression of T cell effector function by IFN-gamma-licensed human mesenchymal stromal cells. *J Immunol.* 2014;192(4):1491–501.
 49. Skovronova R, Grange C, Dimuccio V, Deregibus MC, Camussi G, Bussolati B. Surface marker expression in small and medium/large mesenchymal stromal cell-derived extracellular vesicles in naive or apoptotic condition using orthogonal techniques. *Cells.* 2021;10(11):2948.
 50. Eleuteri S, Fierabracci A. Insights into the Secretome of Mesenchymal Stem Cells and Its Potential Applications. *Int J Mol Sci.* 2019;20(18):4597.
 51. Yan W, Diao S, Fan Z. The role and mechanism of mitochondrial functions and energy metabolism in the function regulation of the mesenchymal stem cells. *Stem Cell Res Ther.* 2021;12(1):140.
 52. Moll G, Ankrum JA, Kamhieh-Milz J, Bieback K, Ringden O, Volk HD, et al. Intravascular mesenchymal stromal/stem cell therapy product diversification: time for new clinical guidelines. *Trends Mol Med.* 2019;25(2):149–63.
 53. Fischer UM, Harting MT, Jimenez F, Monzon-Posadas WO, Xue H, Savitz SJ, et al. Pulmonary passage is a major obstacle for intravenous stem cell delivery: the pulmonary first-pass effect. *Stem Cells Dev.* 2009;18(5):683–92.
 54. Eggenhofer E, Benseler V, Kroemer A, Popp FC, Geissler EK, Schlitt HJ, et al. Mesenchymal stem cells are short-lived and do not migrate beyond the lungs after intravenous infusion. *Front Immunol.* 2012;3:297.
 55. de Witte SFH, Luk F, Sierra Parraga JM, Gargasha M, Merino A, Korevaar SS, et al. Immunomodulation by therapeutic mesenchymal stromal cells (MSC) is triggered through phagocytosis of MSC by monocytic cells. *Stem Cells.* 2018;36(4):602–15.
 56. Prockop DJ. Repair of tissues by adult stem/progenitor cells (MSCs): controversies, myths, and changing paradigms. *Mol Ther.* 2009;17(6):939–46.
 57. Galleu A, Riffo-Vasquez Y, Trento C, Lomas C, Dolcetti L, Cheung TS, et al. Apoptosis in mesenchymal stromal cells induces in vivo recipient-mediated immunomodulation. *Sci Transl Med.* 2017;9(416):eaam7828.
 58. Braza F, Dirou S, Forest V, Sauzeau V, Hassoun D, Chesne J, et al. Mesenchymal stem cells induce suppressive macrophages through phagocytosis in a mouse model of asthma. *Stem Cells.* 2016;34(7):1836–45.
 59. Pang SHM, D'Rozario J, Mendonca S, Bhuvan T, Payne NL, Zheng D, et al. Mesenchymal stromal cell apoptosis is required for their therapeutic function. *Nat Commun.* 2021;12(1):6495.

Publisher's Note

Springer Nature remains neutral with regard to jurisdictional claims in published maps and institutional affiliations.

Ready to submit your research? Choose BMC and benefit from:

- fast, convenient online submission
- thorough peer review by experienced researchers in your field
- rapid publication on acceptance
- support for research data, including large and complex data types
- gold Open Access which fosters wider collaboration and increased citations
- maximum visibility for your research: over 100M website views per year

At BMC, research is always in progress.

Learn more biomedcentral.com/submissions

